JOURNAL OF Applied Polymer SCIENCE

Preparation and Swelling Behaviors of Porous Hemicellulose-*g*-Polyacrylamide Hydrogels

Xiao-Feng Sun, Zhanxin Jing, Guangzheng Wang
Ministry of Education Key Laboratory of Applied Physics and Chemistry in Space, College of Science, Northwestern Polytechnic University, Xi'an 710072, China
Correspondence to: X.-F. Sun (E-mail: xf001sn@nwpu.edu.cn)

ABSTRACT: Novel porous hydrogels were successfully synthesized from hemicelluloses (HCs) and acrylamide (Am) with poly(ethylene glycol) (PEG) as the porogen. The prepared hydrogels were characterized by Fourier transform infrared spectroscopy, thermogravimetric analysis, and scanning electron microscopy (SEM). The results show that the used PEG was not involved in the formation process of the hydrogels, and the HC-*g*-polyacrylamide hydrogels displayed a higher thermal stability than the hemicellulosic polymer. SEM analysis confirmed that the prepared hydrogels had porous structures. The effects of the Am/HC ratio, the amount and molecular weight of PEG and the amount of the crosslinker *N,N*-methylene bisacrylamide on the swelling ratio of the prepared hydrogels were investigated in detail. The experimental data were fitted with the exponential heuristic equation and the Schott second-order dynamic equation. The diffusion of water molecules into the hydrogel network was found to be non-Fickian in behavior, and the swelling kinetics could be described by the Schott second-order dynamic equation. © 2012 Wiley Periodicals, Inc. J. Appl. Polym. Sci. 000: 000–000, 2012

KEYWORDS: biomaterials; gels; swelling

Received 26 April 2012; accepted 22 June 2012; published online
DOI: 10.1002/app.38240

INTRODUCTION

Hydrogels are three-dimensional network structural materials, and they can swell in water but do not dissolve in water.[1,2] According to their sensitivity to different environmental factors, hydrogels can be divided into pH-sensitive, thermosensitive, magnetic-sensitive hydrogels, and so on. Because hydrogels respond to some minor changes in the external environment, they have been widely used in biomedical engineering,[3] tissue engineering,[4] and medical carriers.[5,6] However, the swelling rate of hydrogels synthesized with traditional methods is lower, and this greatly restricts the applications of hydrogels in drug delivery, transmission, tissue engineering, and other biomedical applications.[7]

In recent years, porous hydrogels have attracted much attention because of their excellent swelling and response properties. Hydrogels with porous structures offer a way for water molecules to enter the hydrogel network; this greatly improves the response of the hydrogel. In accordance with its pore-forming mechanism, the preparation method of porous hydrogels can be divided into the freeze-drying method, foaming agents method, porogen method, template method, phase separation, and so on.[7,8] Chitosan–poly(ethylene oxide) semi-interpenetrating network hydrogels with a porous matrix were prepared with the freeze-drying method, and the result indicates that this hydrogel could be useful for the localized delivery of antibiotics in the acidic environment of gastric fluid.[9] The porogen method uses porogens, such as poly(ethylene glycol) (PEG), NaCl, glucose, $CaCO_3$, and silicone in the formation process of hydrogels.[7,8] Macroporous poly(acrylamide-*co*-sodium methacrylate) superabsorbent hydrogels were prepared with glucose as the porogen, and the researchers found that the number of pore channels on the hydrogel surface increased with increasing concentration of the porogen solution that was used for the polymerization reactions.[8] Zhang et al.[10] prepared poly(*N*-isopropyl acrylamide-*co*-acrylic acid) hydrogels with PEG as the porogen, and the result suggests that the porous hydrogels exhibited faster response rates than conventional hydrogels. In recent years, porous hydrogels have demonstrated potential applications in tissue engineering and drug delivery compared to traditional hydrogels. For example, Risbud et al.[11] prepared porous pH-sensitive chitosan–poly(vinyl pyrrolidone) hydrogels by the freeze-dried method, and the result indicates that the hydrogels could serve as potential candidates for antibiotic delivery in an acidic environment. Loebsack et al.[12] prepared porous hydrogel beads from sodium algiate and arginine-glycine-aspartate (RGD) peptides using the foaming agents method, and the hydrogel beads had the desired properties for the development of soft-tissue-engineering construction.

Also interesting in the preparation of hydrogels is the introduction of natural polysaccharides. Hemicelluloses (HCs) are rich, inexhaustible, and renewable polysaccharides, and they are only the second to cellulose in content in plant resources,[13] which account for one-fourth to one-third of plant resources.[14] HCs have excellent hydrophilicity, biodegradability, and biocompatibility; therefore, materials based on HCs would have broad prospects. HCs are generally defined as the alkaline soluble material remaining after the removal of pectin substances, and they are made of D-xylose, L-arabinose, D-glucose, D-galactose, D-mannose, D-glucuronic acid, 4-*O*-methyl-D-glucuronic acid, D-galacturonic acid, and a small amount of L-rhamnose and L-fucose.[13–16]

Novel porous hydrogels based on wheat straw HCs were synthesized in this study, and PEG was embedded in the hydrogels during the polymerization process as a porogen and was removed by washing with distilled water after hydrogel formation. Compared to traditional hydrogels, the HCs-based porous hydrogel had many advantages, such as nontoxicity, biocompatibility, biodegradability, and an anticancer effect, and they should have potential applications in biomedical fields. The synthesized hydrogels were characterized by Fourier transform infrared (FTIR) spectroscopy, thermogravimetric analysis (TGA), and scanning electron microscopy (SEM), and the effects of the Am/HC ratio, PEG, and *N,N*-methylene bisacrylamide (Bis) on the swelling ratio were studied. The exponential heuristic equation and the Schott second-order dynamic equation were used to analyze the swelling mechanism of the prepared hydrogels.

EXPERIMENTAL

Materials

The monomer acrylamide (Am) was purchased from Tianjin Kermel Chemical Reagent Co. (Tianjin, China). The Bis crosslinker and the ammonium persulfate (APS) initiator were purchased from Tianjing Hongyan Chemical Reagent Factory (Tianjin, China). The PEG porogen was purchased from J&K Chemical, Ltd (Tianjin, China). All other reagents used were analytical grade.

Isolation of HC from Wheat Straw

HC was isolated from wheat straw with the following treatment steps: (1) wheat straw was dewaxed with toluene and ethanol at a volume ratio of 2 : 1 in a Soxhlet extractor for 12 h; (2) after filtration, the residue was delignified with sodium chlorite in acidic solution (pH 4.0) at 75°C for 2 h to obtain holocellulose; and (3) the holocellulose was treated with 10% KOH with a solid to liquid ratio of 1 : 20 at room temperature for 10 h and then filtered to separate HC and cellulose. The filtrate was neutralized to pH 5.5, concentrated at reduced pressure, and then precipitated in 3 volumes of ethanol, and finally, pure HC was obtained for further use. The sugar composition of the isolated HC was determined by gas chromatography, and we found that the isolated HC contained 80.4% xylose and 12.5% arabinose (relative to the total sugar content).

Preparation of the Porous HC-*g*-Polyacrylamide (PAAm) Hydrogels

The porous HC-*g*-PAAm hydrogels were prepared by free-radical polymerization. HC (0.5 g) and a certain amount of PEG were dissolved in distilled water (10 mL) in a beaker that was fitted with a magnetic stirrer and placed in a water bath at 45°C. Thereafter, the APS initiator (0.05 g) was added to the mixed solution to produce free radicals, and variable amounts of Am and the Bis crosslinker were also added in time. The mixed solution was vigorously stirred for 5 min, and then, the beaker was sealed and put in a water bath at 45°C for 1 h without stirring. The prepared hydrogels were taken out and cut into uniform sized pieces, and these pieces were immersed in distilled water for 2 days. During this period, it was necessary to change the water regularly to wash away the unreacted monomer and PEG. Finally, the prepared hydrogels were placed in an oven and dried to a constant weight. The feed compositions of the hydrogels are specified in Table I.

Table I. Feed Composition of the Porous HC-*g*-PAAm Hydrogels

Sample code	Am/HC (g/g)	PEG6000 (%)[a]	PEG1500 (%)[a]	Bis (g)
Gel-1	4	10		0.050
Gel-2	6	10		0.050
Gel-3	8	10		0.050
Gel-4	10	10		0.050
Gel-5	8	0		0.050
Gel-6	8	5		0.050
Gel-7	8	20		0.050
Gel-8	8		10	0.050
Gel-9	8	10		0.025
Gel-10	8	10		0.075
Gel-11	8	10		0.100

[a]PEG (wt %) = PEG/(HC + Am).

Characterization

The dried hydrogel samples were analyzed with an FTIR spectrometer (Nicolet 510, USA) within the frequency range 4000–400 cm^{-1} after the samples were milled, mixed with KBr, and laminated. Approximate 10 mg of dried sample was milled and placed in a TGA instrument (model TGA/SDTA851[e], USA), which was heated from 25 to 600°C under nitrogen with a flow rate of 40 mL/min and a heating rate of 20 K/min. To determine the morphologies of the prepared hydrogels, the swollen hydrogels were freeze-dried, coated with gold, and then analyzed by SEM (S-2460N, Hitachi, Tokyo, Japan).

Swelling Tests

A known mass of the hydrogel sample was immersed in 100 mL of distilled water at room temperature. After certain time intervals, the hydrogel was taken out and weighed after removal of excess water on the surface. All tests on the swelling ratio of the samples were conducted in triplicate. The swelling ratios at time t was calculated with the following equation:

$$S_t(\mathrm{g/g}) = \frac{(W_t - W_d)}{W_d} \quad (1)$$

where W_t(g) is the weight of the swollen hydrogel at time t (min) and W_d(g) is the weight of the dry hydrogel.

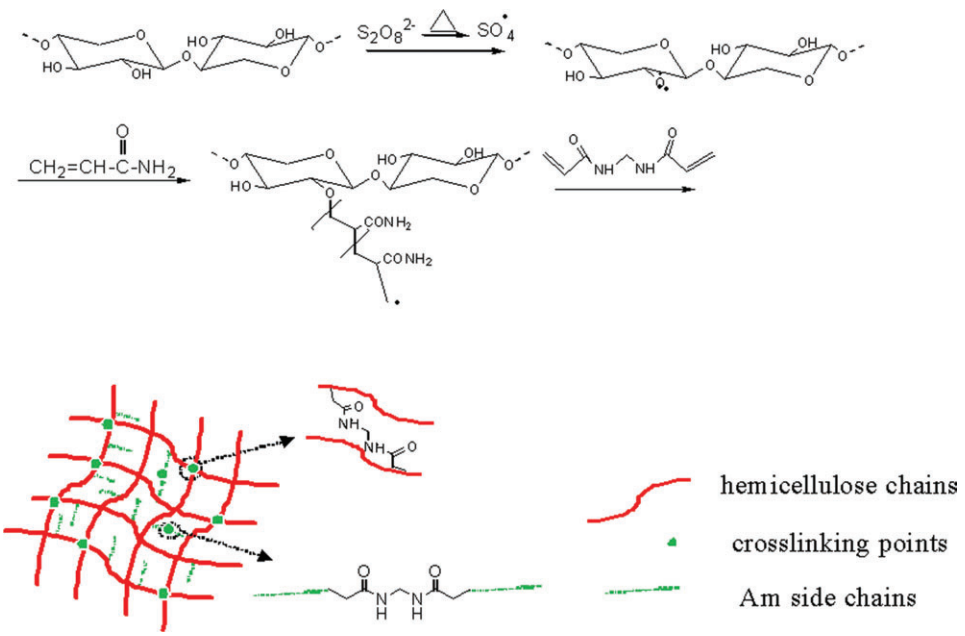

Figure 1. Proposed mechanism for the synthesis of the porous HC-*g*-PAAm hydrogels. [Color figure can be viewed in the online issue, which is available at www.interscience.wiley.com.]

RESULTS AND DISCUSSION

Preparation of the HC-*g*-PAAm Hydrogels

The proposed mechanism for the synthesis of the porous HC-*g*-PAAm hydrogels is shown in Figure 1. The APS initiator produced sulfate anion radicals under the conditions used here because of thermal decomposition, and sulfate anion radical abstracted hydrogen from the hydroxyl groups of HC to form corresponding alkoxyl radicals, which could act as active sites capable of grafting Am onto HC. The added Bis crosslinker could also react with two active sites to form the hydrogel network. In the hydrogel preparation process, PEG was added and embedded into the hydrogels, but it did not participate in the polymerization reaction. After the formation of hydrogels, PEG was removed by washing with distilled water.

FTIR Analysis

FTIR spectroscopy is an important analysis tool, and it is used to determine the presence of some functional groups by their characteristic adsorption peaks. Figure 2 shows the IR spectra of HC, gel-3, gel-5, and PEG. The bands at 3049, 2923, 1637, 1044, and 894 cm^{-1} were the characteristic adsorptions of HC.[16] The broad band at 3409 cm^{-1} was attributed to the stretching of hydroxyl groups, and the band at 2923 cm^{-1} arose from the C—H stretching vibration of methyl and methylene. The peak at 1637 cm^{-1} was assigned to the adsorbed water. The wave-number characterization for typical xylan was at 1044 cm^{-1}; this was attributed to the C—O and C—C stretching and the glycosidic linkage [V(C—O—C)] contributions.[17] The sharp absorption peak at 894 cm^{-1} was assigned to the frequency vibrations of the C1 group and pyranose ring; this was the characteristic absorption peak of the glycosidic bond between sugar units.[18] Compared to the IR spectrum of HC, the IR spectra of the hydrogels had two significant adsorption peaks at 1648 and 1324 cm^{-1}; these were the characteristic adsorptions of the amide bond, and the band at 1648 cm^{-1} was assigned to the stretching vibration of C=O.[20] The peak at 1324 cm^{-1} was attributed to the stretching vibration of C—N.[20] The IR spectra of gel-3 and gel-5 were enlarged in the range 1800–800 cm^{-1}, and the IR spectrum of gel-3 was consistent with that of gel-5 and did not show the typical absorption peaks for PEG.[21] These result reveal that the PEG molecule only acted as a porogen during the polymer crosslinking process, did not participate in the crosslinking reaction, and was removed by the water washing after the reaction.

TGA

The thermal properties of a material are essential to study for its applications, and they are directly related to the composition

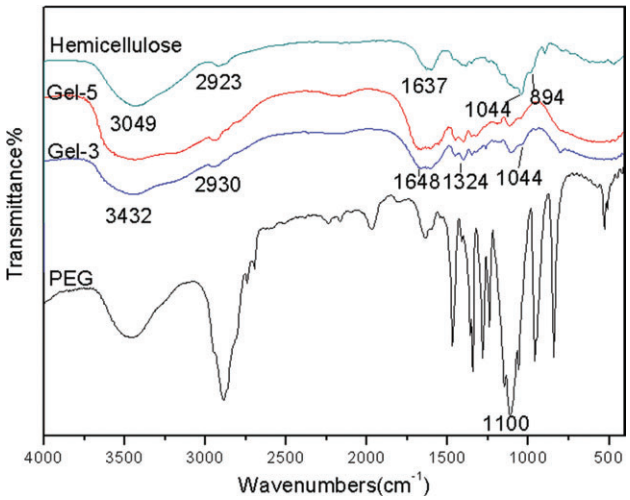

Figure 2. FTIR spectra of the HC, PEG, gel-3, and gel-5. [Color figure can be viewed in the online issue, which is available at www.interscience.wiley.com.]

Applied Polymer SCIENCE

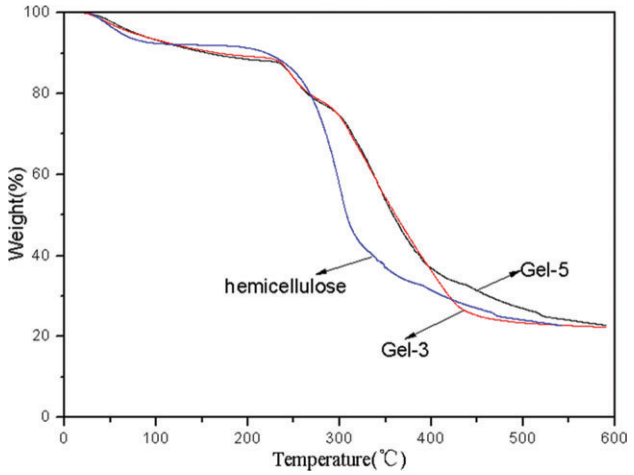

Figure 3. TG curves of HC, gel-3, and gel-5. [Color figure can be viewed in the online issue, which is available at www.interscience.wiley.com.]

of a material. TGA is generally used to analyze the thermal stability of a material. The TGA curves of HC, gel-3, and gel-5 are displayed in Figure 3. It can be seen from Figure 3 that the TGA curve of gel-3 was basically consistent with that of gel-5; it also indicates that the porogen in gel-3 was completely removed and not involved in the polymerization process. TGA also showed that the prepared hydrogels were more thermally stable than HC, as the maximum decomposition temperatures of the hydrogels and HC were at 350 and 300°C, respectively. The TGA curves of the two hydrogels showed that their decomposition underwent three stages on the whole. The first stage was caused by the loss of bound water in temperature range from 50 to 200°C. The second stage, in the range from 200 to 300°C, was due to the dehydration and decarboxylation of hydrogels. The final stage was attributed to the degradation of the remaining polymer chains in the range from 300 to 600°C.

Morphological Analysis of the Porous Hydrogels

The morphologies of the prepared hydrogels were analyzed by SEM, and the SEM images are shown in Figure 4. It can be seen from Figure 4(a–c) that the prepared hydrogels had interconnected pore channels, and the interconnected pore channels of gel-1 were slightly larger than those of the other hydrogels. This was due to the decreases in chain winding and hydrogen-bond forces in the hydrogels with higher HC contents. Figure 4(a,b) also shows large amounts of small pores on the cross sections of the hydrogels, and this may have been due to the action of PEG. It can be observed from Figure 4(d–f) that the cross section of gel-5 was dense, and there was no obvious pore structure, whereas the other hydrogels had large amounts of pores, and their pore size was uniform. This resulted from the formation of the pores after the removal of PEG. Because the preparation of porous hydrogels with the porogen method mainly depends on the memory effect, which produces pores after the removal of the porogen,[7,8] the pore size is related to the volume or molecular weight of the porogen. Therefore, we observed that the pore size of gel-3 was larger than that of gel-8 because gel-3 used PEG 6000 as a porogen, whereas gel-8 used PEG 1500 as a porogen. Similar results were reported for macroporous poly(*N*-isopropyl acrylamide-*co*-acrylic acid) hydrogels and fast-responding pH-/temperature-sensitive poly(*N*-isopropyl acrylamide)/sodium alginate hydrogels.[10]

Effect of the Am/HC Ratio on the Swelling Ratio

The swelling ratio of the hydrogels mainly depends on the feed compositions, which are directly related to the elasticity of the hydrogel network, the average pore size, and the pore distributions within the hydrogel.[22] The effects of the monomer Am/HC ratio, the amounts of the used PEG, the PEG molecular weight, and the Bis crosslinker on the swelling capacity of the hydrogels were examined.

The Am/HC feed ratio was varied from 4 to 10 to study its effect on the swelling ratios of the hydrogels. The acquired results are shown in Figure 5, and the swelling ratio of the samples decreased as the Am/HC ratio increased. Figure 4 shows that the interconnected pore channels were smaller in the hydrogels with higher Am/HC ratios. This may have been due to the increased number of hydrogen bonds in the hydrogel network and the enhanced homopolymerization reaction over graft copolymerization at higher Am/HC ratios. Analogous results were observed in carboxymethylcellulose-*g*-PAAm.[23] In contrast, the increase of the proportion of hydrophilic polymer HCs in the hydrogels took advantage of the diffusion of water into the hydrogel network and resulted in a higher swelling ratio.

Effect of the Amount of PEG on the Swelling Ratio

We studied the effect of the amount PEG used on the swelling ratio of the prepared hydrogels by varying the percentage of added PEG from 0 to 20 wt %, and the acquired results are displayed in Figure 6. As shown, the swelling ratio of the hydrogels increased as the added percentage of PEG increased from 0 to 10%, and the swelling ratio of the porous hydrogel was 1.69 times of that of the conventional hydrogel (gel-5). As shown in Figure 6, the porosity of the hydrogel increased with increasing amount of the PEG used; this led to an increase in the surface area of the hydrogel. Thus, the swelling ratio increased. However, the swelling ratio of the hydrogels decreased when the added PEG percentage increased from 10 to 20%. One reason was that PEG may have joined the polymerization reaction when it was excessive, and the other reason was that large amounts of porogen may have destroyed the structure of the hydrogels. These affected the swelling ratio of the hydrogels. Similar behavior was reported in porous dextran microspheres with dimethyl ether of PEG as the porogen.[24]

Effect of the Molecular Weight of PEG on the Swelling Ratio

Porous hydrogels that are prepared with the porogen method mainly take advantage of the memory effect of the hydrogel, and the produced hole does not vanish after the removal of the porogen.[7] The pore size of the hydrogel is related to the molecular weight of the porogen.

The effects of PEG6000 and PEG1500 on the swelling ratio of the prepared hydrogels were studied, and the results are shown in Figure 7. We found that the swelling ratio of gel-3 was higher than that of gel-8, and this was because gel-3 used PEG6000 as the porogen and had a larger pore size and surface area; this created a chance for the interaction between the water

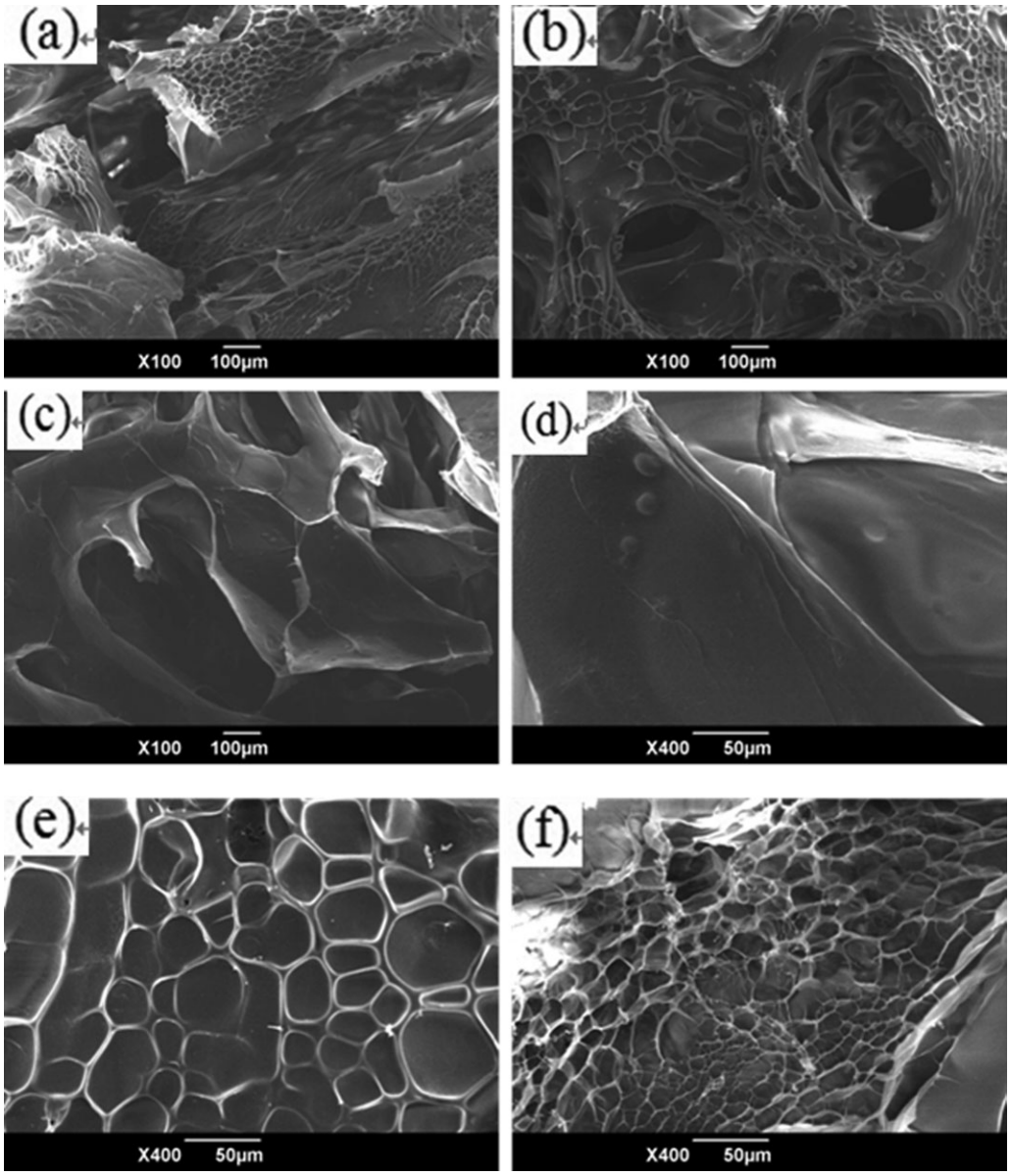

Figure 4. SEM images of the cross-sectional morphology of the hydrogels: (a) gel-1 × 100, (b) gel-3 × 100, (c) gel-5 × 100, (d) gel-5 × 400, (e) gel-3 × 400, and (f) gel-8 × 400.

molecules and the hydrophilic groups of the hydrogel. However, PEG1500 was added in the preparation process of gel-5, and the pore size and surface area of gel-5 was smaller than that of gel-3. This impeded the integration between the hydrophilic groups and water molecules, which led to a decrease in the swelling ratio. This result was consistent with those of poly(*N*-isopropyl acrylamide)/sodium alginate hydrogels and macroporous PAAm hydrogels that were prepared with PEG.[11,25]

Effect of the Amount of the Bis Crosslinker on the Swelling Ratio

The effects of the amount of the Bis crosslinker on the swelling ratio of the prepared hydrogels are displayed in Figure 8, and the swelling ratios of the samples decreased sharply as the amount of crosslinker was increased from 0.025 to 0.100 g. The hydrogels had a lower crosslink density at lower Bis feeds, whereas the crosslinking density of the hydrogels that were synthesized with the high amount of crosslinking agent increased; this produced a dense network structure and enhanced the elastic contraction of the hydrogels. This led to a reduction in the space between the polymer chains and restricted the penetration of water molecules into the hydrogels. Thus, the swelling ratio decreased. We also observed that the required time of swelling equilibrium decreased with increasing Bis amount, and this may have been because the hydrogel network was dense and inflexible, and the hydrogel achieved swelling equilibrium with lower water sorption. These results were reported for sodium alginate-*g*-poly(sodium acrylate)/poly(vinyl pyrrolidone) semi-interpenetrating network hydrogels and xylan-rich HCs-*g*-acrylic acid ionic hydrogels.[18,26]

Applied Polymer SCIENCE

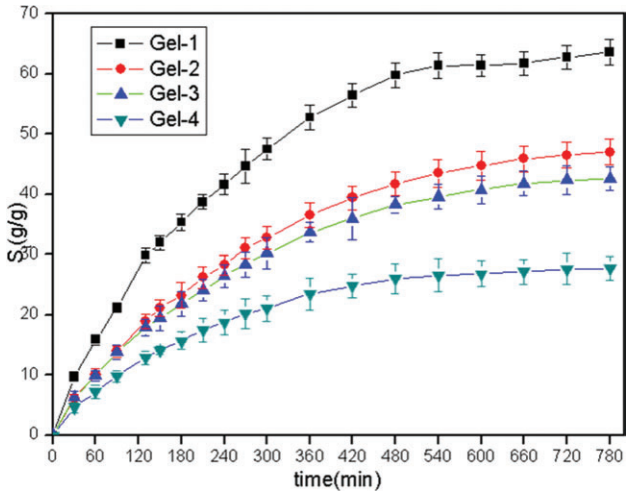

Figure 5. Effect of the Am/HC ratio on the swelling ratio of the hydrogels. [Color figure can be viewed in the online issue, which is available at www.interscience.wiley.com.]

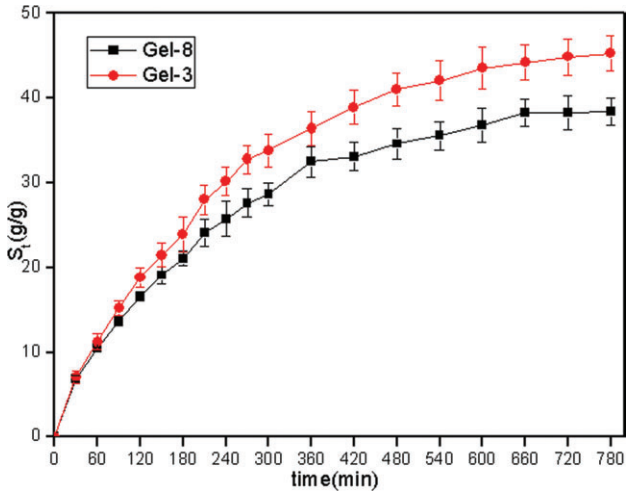

Figure 7. Effect of the molecular weight of PEG on the swelling ratio of the hydrogels. [Color figure can be viewed in the online issue, which is available at www.interscience.wiley.com.]

Analysis of the Swelling Kinetics

Studies of the swelling kinetics of hydrogels are important for their applications in the biomedical, pharmaceutical, environmental, and agricultural fields.[27] To explain the swelling mechanism of the prepared hydrogels, two empirical equations, the exponential heuristic equation and the Schott second-order dynamic equation, were used to analyze the experimental data.

The exponential heuristic equation is generally used to study the diffusion mechanism of water molecules in a hydrogel network during the initial swelling process.[28] It can be written as follows:[27–29]

$$F = \frac{S_t}{S_\infty} = kt^n \tag{2}$$

Equation (2) can be reformed into eq. (3):

$$\ln \frac{S_t}{S_\infty} = \ln k + n \ln t \tag{3}$$

where F is the fractional uptake; S_t is the amount of absorbed water at time t (min); S_∞ is the maximum amount of absorbed water; k is a constant incorporating the characteristics of the polymer network and the solvent, and n is the diffusion exponent, which is indicative of the transport mechanism. The value of n indicates the swelling mechanism of the hydrogels. The swelling process follows Fickian diffusion when n is less than 0.5; this is determined by solvent diffusion. When $0.5 < n < 1$, the swelling process follows non-Fickian diffusion; this is the result of the combined effect of solvent diffusion and the relaxation of macromolecular chains. Swelling is mainly decided by the relaxation of macromolecular chains when n is greater than 1.[30,31]

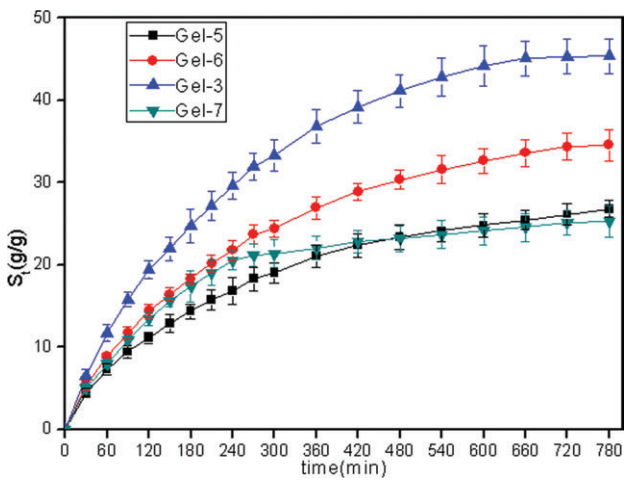

Figure 6. Effect of the amount of PEG on the swelling ratio of the hydrogels. [Color figure can be viewed in the online issue, which is available at www.interscience.wiley.com.]

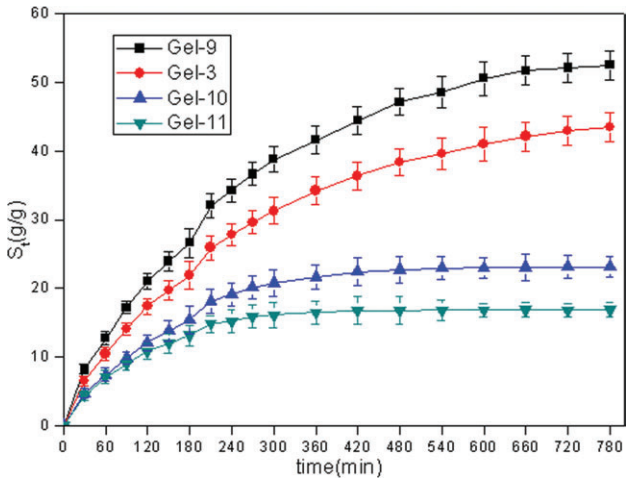

Figure 8. Effect of the amount of crosslinker Bis on the swelling ratio of the hydrogels. [Color figure can be viewed in the online issue, which is available at www.interscience.wiley.com.]

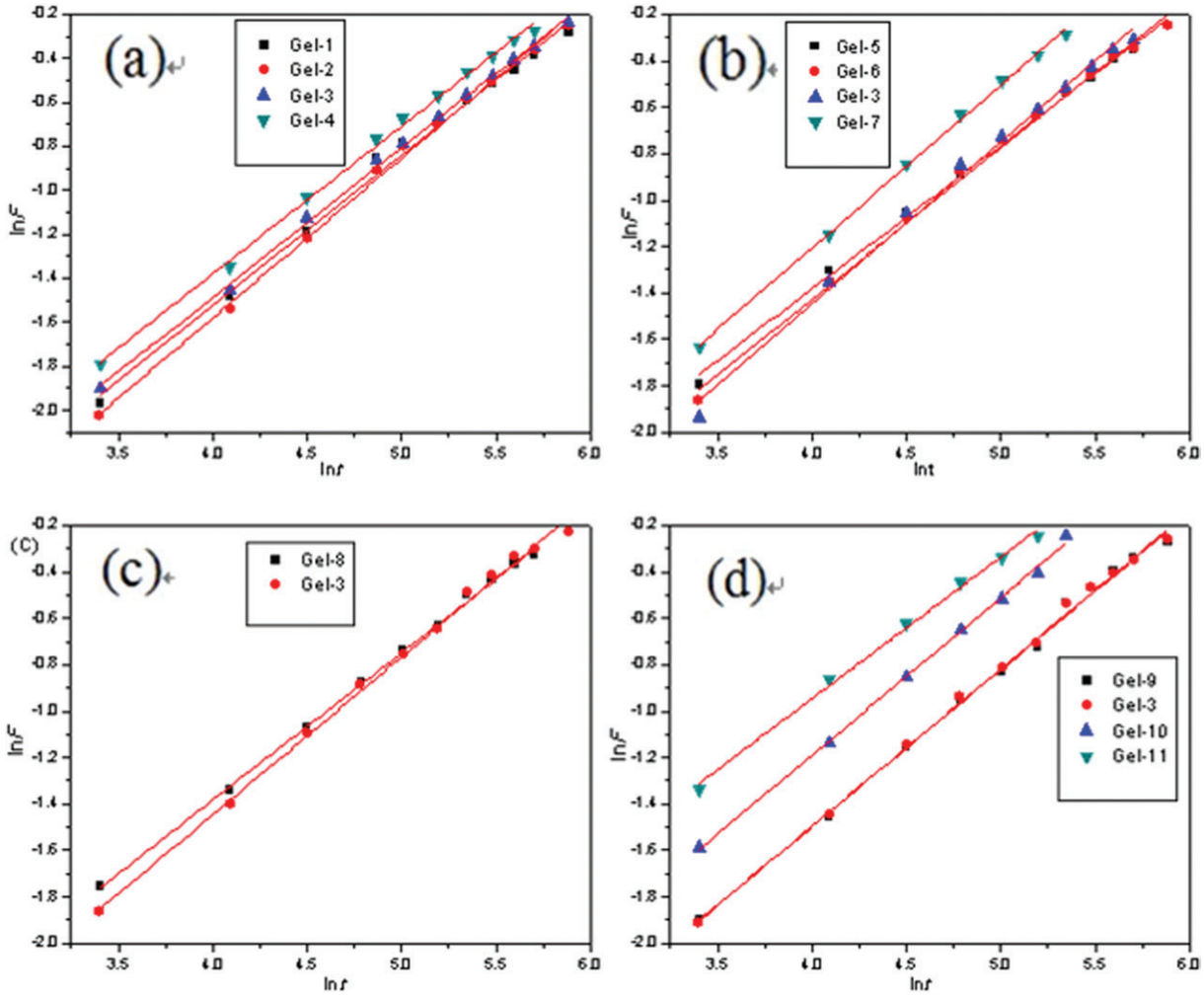

Figure 9. ln F as a function of ln t: (a) hydrogels with different Am/HC ratios, (b) hydrogels with different amounts of the porogen PEG, (c) hydrogels with different PEG molecular weights, and (d) hydrogels with different amounts of the Bis crosslinker. [Color figure can be viewed in the online issue, which is available at www.interscience.wiley.com.]

We plotted ln F versus ln t, and the acquired graphs are shown in Figure 9. The values of n and k obtained from the profile of ln F versus ln t are listed in Table II, where n is the slope of curve and k was calculated by the intercept. According to Table II, the n values of all of samples were between 0.5 and 1. This indicated that the swelling of the hydrogels was mainly determined by the water spread and coordinated relaxation of the hydrogels; this revealed that the swelling kinetics of all of the samples did not meet to Fickian diffusion. This was because Fickian diffusion belongs to the first-order dynamic equation, which assumes that the diffusion coefficient and film thickness in the swelling process do not change. However, the volume changed as the hydrogels swelled.

To better understand the swelling mechanism of the prepared hydrogels, the extensive swelling process was studied by the Schott second-order dynamic equation. It is described with the following equation:[32,33]

$$\frac{t}{S} = A + Bt \tag{4}$$

Table II. Kinetic Parameters of Hydrogel Swelling in Distilled Water

Factor	Variable	R^2	n	k
Am/HC ratio	4	0.9937	0.6845	0.0141
	6	0.9973	0.7266	0.0113
	8	0.9981	0.6781	0.0150
	10	0.9976	0.6723	0.0171
Amount of PEG	0%	0.9975	0.6182	0.0212
	5%	0.9935	0.6503	0.0144
	10%	0.9906	0.6974	0.0162
	20%	0.9987	0.7015	0.0181
PEG molecular weight	1500	0.9987	0.6340	0.0199
	6000	0.9964	0.6795	0.0155
Amount of crosslinker	0.025	0.9965	0.6763	0.0149
	0.050	0.9975	0.6779	0.0150
	0.075	0.9980	0.6789	0.0201
	0.100	0.9955	0.6105	0.0338

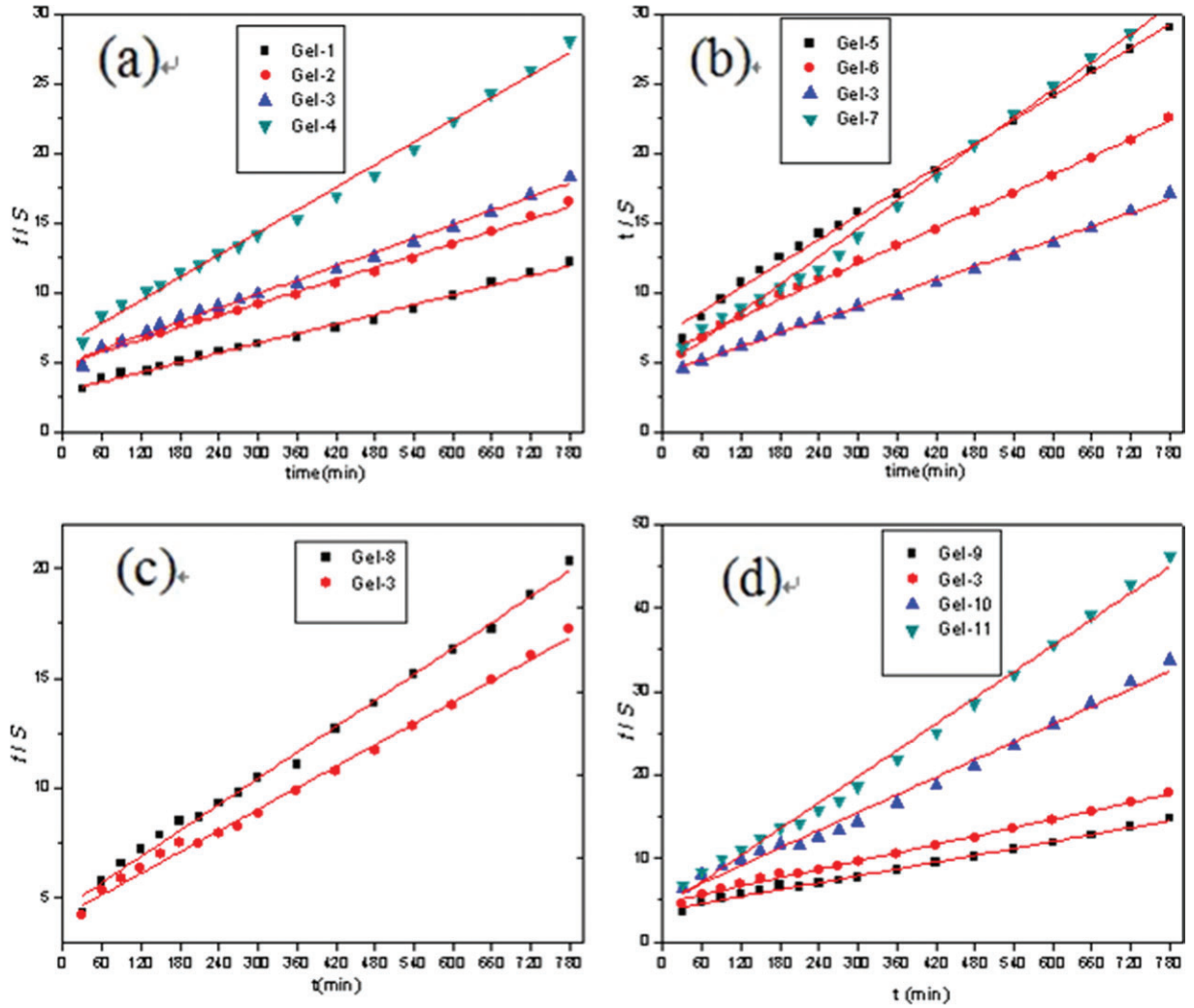

Figure 10. t/S as a function of time: (a) hydrogels with different Am/HC ratios, (b) hydrogels with different amounts of porogen PEG, (c) hydrogels with different PEG molecular weights, and (d) hydrogels with different amounts of the Bis crosslinker. [Color figure can be viewed in the online issue, which is available at www.interscience.wiley.com.]

where A and B are constants and are explained as follows: when the swelling process continued for a longer period, $Bt \gg A$. According to eq. (4), $B = 1/S_\infty$, that is, B is the reciprocal of the maximum swelling ratio. In contrast, when $A \gg Bt$, the swelling process was shorter, and eq. (4) could be reformed as follows:

$$\lim_{t\to 0}\frac{dS}{dt} = \frac{1}{a} \tag{5}$$

where a is the reciprocal of the initial swelling rate (r_0).

The t/S versus t graph was fitted, and the results are displayed in Figure 10. The calculated kinetic parameters are listed in Table III. As shown in Table III, the R^2 values of all of the samples were greater than 0.98, and the experimental swelling ratio (S^b_∞) was very close to the maximum theoretical swelling ratio (S^a_∞). This indicated that the swelling process of the hydrogels followed the Schott second-order dynamic equation. It can also be found from Table III that the effects of the Am/HC ratio, the amount of PEG used, the molecular weight of PEG, and the amount of the Bis crosslinker on r_0 were in agreement with the experimental results shown in Figures 5–8.

The r_0 value decreased from 0.3459 to 0.1608 g of water (g gel)$^{-1}$ min^{-1} as the Am/HC ratio increased from 4 to 10. This was because the HC chains had less freedom for chain relaxation at higher Am/HC ratios, and this could have impeded the diffusion rate of the water molecules. The HC content continuously decreased with increasing Am/HC ratio; this enhanced the compact arrangement of the hydrogel network. Thus, the diffusion of water molecules into the hydrogel network became difficult.[23,29]

When the amount of added PEG was increased, the porosity of the hydrogels increased. It was very clear that r_0 increased as the added percentage of PEG rose from 0 to 10%. However, the r_0 value decreased when the amount of PEG was increased to 20%, and this may have been because more PEG molecules participated in hydrogel formation, so the porosity of the hydrogels decreased.

Table III. r_0, S^b_∞, S^a_∞, and Rate Constant (k_s) Values of the Hydrogels in Distilled Water

Factor	Variable	R^2	S^a_∞ (g of water/g of gel)	S^b_∞ (g of water/g of gel)	r_0 [g of water (g of gel)$^{-1}$ min^{-1}]	$k_s \times 10^4$ [g of water (g of gel)$^{-1}$ min^{-1}]
Am/HC ratio	4	0.9930	65.50	73.95	0.3459	0.8062
	6	0.9945	48.32	47.55	0.2056	0.8806
	8	0.9945	43.63	43.18	0.2032	1.0679
	10	0.9944	28.58	27.76	0.1608	1.9682
Amount of PEG	0%	0.9967	26.62	26.83	0.1441	2.034
	5%	0.9975	34.90	34.56	0.1768	1.4512
	10%	0.9970	46.77	45.38	0.2381	1.0887
	20%	0.9957	25.51	25.28	0.2173	3.3392
PEG molecular weight	1500	0.9952	39.31	39.89	0.2246	1.4533
	6000	0.9951	46.30	45.77	0.2393	1.1165
Amount of crosslinker	0.025	0.9932	53.72	55.75	0.2631	0.9115
	0.050	0.9956	44.07	44.40	0.2129	1.0960
	0.075	0.9891	24.05	23.13	0.2031	3.5107
	0.100	0.9939	17.35	16.93	0.1949	8.0442

We observed that the r_0 values of the hydrogels that were prepared with PEG1500 and PEG6000 as porogens were 0.2246 and 0.2394 g of water (g gel)$^{-1}$ min^{-1}, respectively. This was due to the larger pore size of the hydrogel that was produced with PEG 6000, and it was greatly advantageous for the diffusion of water molecules into the inner part of the hydrogel. The pore size of the hydrogel that was produced with PEG1500 was relatively smaller; therefore, the r_0 value was low.[21]

The effect of the amount of Bis crosslinker on r_0 is also shown in Table III. The r_0 values decreased as the amount of Bis increased from 0.025 to 0.10 g. This was because the high crosslinking density of the hydrogel caused a larger rigidity and intermolecular force, which inhibited the chain relaxation and, therefore, impeded the diffusion of water molecules.[34]

CONCLUSIONS

Novel, porous hydrogels were synthesized successfully from HC and Am by free-radical polymerization in the presence of PEG. FTIR and TGA revealed that PEG was not involved in the formation process of the hydrogels, and the prepared hydrogels showed a higher thermal stability than the HC polymer. SEM analysis showed the pore structures of the hydrogels were related to the amount and molecular weight of added PEG.

A low swelling ratio was observed for the hydrogels that were prepared at higher Am/HC ratios and higher crosslinker amounts. The swelling ratio increased when the added PEG percentage rose from 0 to 10%, and the swelling ratio of the porous hydrogel (gel-3) was 1.69 times of that of the conventional hydrogel (gel-5), but it decreased when the PEG amount was higher than 20%. Moreover, the swelling ratio increased with increasing molecular weight of PEG. The analysis of swelling kinetics showed that the swelling process of the porous HC-*g*-PAAM hydrogels was non-Fickian diffusion, and the Schott second-order dynamic equation could describe the swelling process.

ACKNOWLEDGMENTS

The authors acknowledge the joint financial support of the National Natural Science Foundation of China (grant number 20707016), Graduate Starting Seed Fund and Foundation for Fundamental Research of Northwestern Polytechnical University (grant numbers Z2012160 and NPU-FFR-JC20110274), and New Science Star Project of Shaanxi Province (2012KJXX-10).

REFERENCES

1. Dumitriu, R. P.; Mitchell, G. R.; Vasile, C. *Polym. Int.* **2011,** *60*, 222.
2. Vashist, A.; Gupta, Y. K.; Ahmad, S. *Carbohydr. Polym.* **2012,** *87*, 1433.
3. Eyholzer, C.; Borges de Couraca, A.; Duc, F.; Bourban, P. E.; Tingaut, P.; Zimmermann, T.; Månson, J. A. E.; Oksman, K. *Biomacromolecules* **2011,** *12*, 1419.
4. Yang, M. J.; Chen, C. H.; Lin, P. J.; Huang, C. H.; Chen, W.; Sung, H. W. *Biomacromolecules* **2007,** *8*, 2746.
5. Chang, C.; Duan, B.; Cai, J.; Zhang, L. *Eur. Polym. J.* **2010,** *46*, 92.
6. El-Sherbiny, I. M.; Smyth, H. D. C. *Carbohydr. Res.* **2010,** *345*, 2004.
7. Lu, G.; Yan, Q.; Su, X.; Liu, Z.; Ge, C. *Prog. Chem.* **2007,** *19*, 485.
8. Murali Mohan, Y.; Keshava Murthy, P. S.; Mohana Raju, K. *J. Appl. Polym. Sci.* **2006,** *101*, 3202.

9. Patel, V. R. *Amiji. Pharm. Res.* **1996,** *13*, 588.
10. Zhang, J. T.; Huang, S. W.; Wang, L. L.; Zhuo, R. X. *Chem. J. Chin. Univ.* **2004,** *25*, 2370.
11. Risbud, M. V.; Hardikar, A. A.; Bhat, S. V. *J. Controlled Release* **2000,** *68*, 23.
12. Loebsack, A.; Greene, K.; Wyatt, S.; Culberson, C.; Austin, C.; Beiler, R.; Roland, W.; Eiselt, P.; Rowley, J.; Burg, K.; Mooney, D.; Holder, W.; Halberstadt, C. *J. Biomed. Mater. Res.* **2001,** *57*, 575.
13. Lawther, J. M.; Sun, R.; Banks, W. B. *J. Agric. Food Chem.* **1995,** *43*, 667.
14. Sun, X. F.; Sun, R. C.; Fowler, P.; Baird, M. S. *J. Agric. Food Chem.* **2005,** *53*, 860.
15. Sun, R. C.; Wang, X. Y.; Sun, X. F.; Sun, J. X. *Polym. Degrad. Stab.* **2002,** *78*, 295.
16. Sun, X. F.; Jing, Z.; Fowler, P.; Wu, Y.; Rajaratnam, M. *Ind. Crops Prod.* **2011,** *33*, 588.
17. Sun, R. C.; Tomkinson, J. *Eur. Polym. J.* **2003,** *39*, 751.
18. Peng, X.; Ren, J.; Zhong, L.; Peng, F.; Sun, R. *J. Agric. Food Chem.* **2011,** *59*, 8208.
19. Mandal, B. B.; Kapoor, S.; Kundu, S. C. *Biomaterials* **2009,** *30*, 2826.
20. Dragan, E. S.; Apopei, D. F. *Chem. Eng. J.* **2011,** *178*, 252.
21. Çavkara, T.; Bulut, M.; Demirmic, S.; *Nucl. Instrum. Methods Phys. Res. B* **2007,** *265*, 366.
22. Chang, C.; He, M.; Zhou, J.; Zhang, L. *Macromolecules* **2011,** *44*, 1642.
23. Bajpai, A. K.; Anjali, G. *Carbohydr. Polym.* **2003,** *53*, 271.
24. Dai, C.; Wang, Y.; Hou, X. *Carbohydr. Polym.* **2012,** *87*, 2338.
25. Li, Z.; Lin, J.; Wu, J.; Huang, M.; Lu, Y.; Leng, Q. *Journal of Huagiao University (Nat. Sci.)* **2010,** *31*, 649.
26. Wang, W.; Wang, A. *Carbohydr. Polym.* **2010,** *80*, 1028.
27. Kundakci, S.; Üzüm, Ö.B.; Karadag, E. *React. Funct. Polym.* **2008,** *68*, 458.
28. Luo, Y. L.; Wei, Q. B.; Xu, F.; Chen, Y. S.; Fan, L. H.; Zhang, C. H. *Mater. Chem. Phys.* **2009,** *118*, 329.
29. Nizam El-Din, H. M.; Abd Alla, S. G.; El-Naggar, A. W. M. *Radiat. Phys. Chem.* **2010,** *79*, 725.
30. Dalaran, M.; Emik, S.; Güçlü, G.; İyim, T. B.; Özgümüş, S. *Desalination* **2011,** *279*: 170.
31. Katime, I.; Novoa, R.; Zuluaga, F. *Eur. Polym. J.* **2001,** *37*, 1465.
32. Quintana, J. R.; Valderruten, N. E.; Issa, K. *Langmuir* **1999,** *15*, 4728.
33. Katime, I.; Velada, J. L.; Novoa, R.; Díaz de Apodaca, E.; Puig, J.; Mendizabal, E. *Polym. Int.* **1996,** *40*, 281.
34. Rasool, N.; Yasin, T.; Heng, J. Y. Y.; Akhter, Z. *Polymer* **2010,** *51*, 1687.